to suppose that the development of the unusual crater profiles was related to the ability of the glassy workpieces to deform viscously at relatively low temperatures. This behaviour was presumably possible because there was insufficient time for the workpieces to crystallize during spark erosion. The observations that central columns arose at the crater centres indicated that the spark machining process produced normal forces which pulled the viscous material in the heated workpiece zone towards the other electrode.

The volume of material that deformed was approximately the same for both the non-crystalline and crystalline specimens in spite of the fact that the former were potentially able to deform viscously at low temperatures. It was therefore likely that the formation of the central columns modified the spark discharge characteristics so as to produce less heating of the glassy workpieces. The same feature probably also suppressed the formation of radial discharge pressures [6, 12, 13] at the surface and the attendant displacement of material to form a rim. It can also be tentatively concluded that in order for a significant amount of spark modification to occur it would have been necessary for the central column to be formed at an early stage of the spark discharge, such as during the pre-arc ignition stage when there is thought to be a strong electrostatic field in the inter-electrode gap [8].

The radial corrugations around the crater edges possibly developed as a result of a Rayleigh–Taylor hydrodynamic instability caused by the rapid acceleration of the interface between two viscous liquids (dielectric and heated glass) in the direction of the denser fluid. The acceleration was brought about by the pulling force that created the central column. Moreover, flow constriction during the displacement of material towards the crater centre would have enhanced the degree of corrugation.

References

1. I. A. BUCKLOW and M. COLE, *Met. Rev.* **14** (1969) 103.
2. H. K. LLOYD and R. H. WARREN, *J. Iron Steel Inst.* **203** (1965) 238.
3. F. S. VAN DIJEK and W. L. DUTRE, *J. Phys. (D)* **7** (1974) 879.
4. E. W. GRAY and J. R. PHARNEY, *J. Appl. Phys.* **45** (1964) 667.
5. J. E. GREENE and J. L. GUERRO-ALVEREZ, *Met. Trans.* **5** (1974) 695.
6. *Idem, Trans. ASME* **95B** (1973) 965.
7. D. W. RUDORFF, *Engineers Digest* **10** (1949) 306.
8. M. M. ATTALA, *Bell Syst. Tech. J.* **34** (1955) 203.
9. J. L. SMITH and W. S. BOYLE, **38** (1959) 537.
10. E. M. WILLIAMS, *Trans. Amer. Inst. Elect. Eng.* **71** (1952) 105.
11. M. M. BRUMA, *Bull. Soc. Franc. Elec.* **1** (1960) 840.
12. H. KURAGUGI, *CIRP* **13** (1966) 313.
13. P. KISLINK, *J. Appl. Phys.* **25** (1954) 897.

Received 14 June
and accepted 25 July 1977.

P. G. BOSWELL
Department of Mining and Metallurgical Engineering, University of Queensland, St. Lucia, Australia, 4067.

Amorphous thin films of stainless steel

In recent years it has become clear that non-crystalline metals and alloys can exhibit different physical and electro-chemical properties to equivalent or similar crystalline phases [1]. The extent of these differences can be wide because it is possible to prepare single phase, non-crystalline alloys at compositions which are not stable in the crystalline form. In particular, mention can be made of transition metal–"metalloid" alloys, such as $Fe_{40}Ni_{40}P_{14}B_6$ and $Fe_{80}B_{20}$, prepared as ribbons or foils by rapid quenching from the melt, which have very good and potentially useful "soft" magnetic properties [1, 2]. Recent work [1, 3–5] on the electrochemical properties of similar alloys of the general type Fe–Cr–Ni–P–C suggest that increased corrosion resistance can be obtained in the amorphous phase. Such glassy phases can also be obtained in films and coatings deposited from the vapour by thermal evaporation or sputtering. In many cases it is necessary to form the deposited layer onto a substrate cooled below room temperature, typically to liquid nitrogen or liquid helium temperatures. Amorphous alloy films also have novel and specific properties related to their non-crystalline atomic arrangement, microstructure

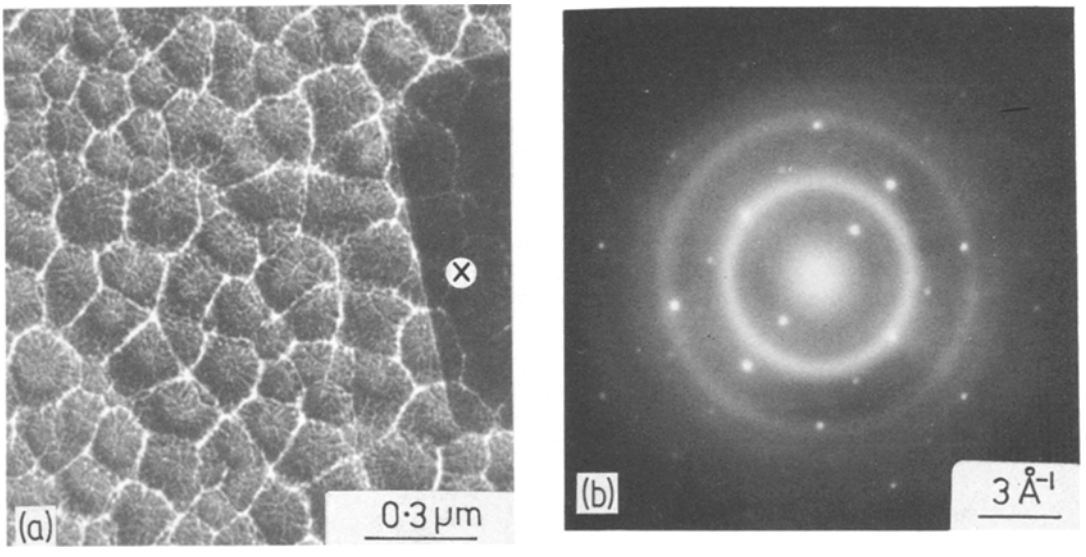

Figure 1 Showing (a) the microstructure and (b) the electron diffraction pattern of a 304 stainless steel film deposited onto a 77 K substrate. The spots are from the super-imposed [2 1 1] oriented NaCl crystal (labelled X) and are used to calibrate the pattern.

and composition [1, 6] and it is possible that, in analogy to the findings by Hashimoto *et al.* [1, 3–5] on non-crystalline foils, non-crystalline coatings of Fe–Cr–Ni alloys may possess attractive corrosion resistant properties. It should also be noted that recent experiments have shown that corrosion resistive [7, 8] and amorphous [9] surface alloys can be prepared by ion implantation techniques.

The purpose of this short paper is to report the preparation of amorphous thin films of the nominal composition of 304 stainless steel (74% Fe, 18% Cr, 10% Ni, < 1% Mn, P, S and Si) sputtered onto crystalline 304 stainless steel and rock-salt substrates. Previous investigations [10, 11] have suggested the formation of a non-crystalline component in sputtered films of stainless steel. Navinsek [10] would seem to describe his microcrystalline films as being "amorphous" and Nowak [11] identified a diffuse electron diffraction maximum amongst crystalline reflections from 304 stainless steel films deposited with additions of Al and Si. Clearly these latter films were structurally inhomogeneous.

The films prepared in this study were deposited in a d.c. bias sputtering unit (based on an Edwards 306 system). The unit was first evacuated to a base pressure of about 5×10^{-7} torr and then flushed out several times with dried argon. The target, a disc of 304 stainless steel, was then pre-sputtered for 15 min in an argon pressure of 2×10^{-2} torr with the substrates shielded. The incoming argon was sputter gettered in an attempt to remove impurities such as N_2, Co_2 and O_2 but no measure of the purity of the gettered argon was attempted. Films were then sputtered with the substrates biased at -120 V and either cooled to 77 K or kept near to room temperature. The deposition rate was about 18 nm min^{-1} and films up to 200 nm thick were grown. During film growth the substrate temperature tended to rise with a typical increase being about 20 K.

The films grown on rock salt were floated onto transmission electron microscope (TEM) support grids and examined in a JEM 200 microscope in imaging and high resolution diffraction modes. Fig. 1 shows the microstructure and diffraction pattern of a typical film deposited at 77 K. The microstructure consists of discrete islands about 150 nm across which are separated by regions of lower density and contain clusters of small particles between about 5 and 15 nm in diameter. The film is assumed to craze into these islands when warming to room temperature because of the difference in thermal expansion coefficients of

TABLE I Normalized positions of diffraction maxima from experimental films and of maxima in calculated structure factors.

Specimen or model	s_1/s_1	s_2/s_1	s_3/s_1	s_4/s_1	s_5/s_1	s_6/s_1	Ref
b c c structure	1	1.41	1.73	2.00	2.24		
crystalline film (a) (this study)	1	1.39	1.72	2.05	2.45		
f c c structure	1	1.16	1.63	1.92	2.0	2.31	
crystalline film (b) (this study)	1	1.21	1.68	2.08	2.48	3.28	
amorphous film (this study)	1	1.68	1.90	2.49			
amorphous Fe film	1	1.69	1.97	2.54			[13]
amorphous Ni film	1	1.70	1.86	2.49			[14]
model 1	1	1.64	1.91	2.50			[15]
model 2	1	1.67	1.84	2.53			[16]

the film and rock-salt substrate. However, this particular microstructure could result from the way the film nucleates and grows on a low temperature substrate [12]. The diffraction pattern of this film is typical of those prepared under similar conditions and consists of a set of diffuse maxima. The normalized values of the scattering parameter $(s = 4\pi \sin\theta/\lambda) s_n/s_1$ at which the maxima occur are listed in Table I. Films deposited onto room temperature substrates gave a diffraction pattern typical of a small grained, crystalline structure, as shown in Fig. 2. An estimate of the grain size from diffraction line broadening is ~1 nm and no evidence of crazing or growth into island clusters was observed in these films. The normalized values of the diffraction rings s_n/s_1, in these films are also given in Table I, (a) neglecting the first maximum and (b) including the first maximum. The extent of agreement and points of difference between these ratios and the calculated values for b c c and f c c crystal structures suggest the crystalline films have a two phase structure.

The diffraction patterns for the amorphous films are typical of those from non-crystalline metals and alloys and are characterized by a prominent first maximum and a split second maximum. The contrast between this pattern and that for the mixed phase crystalline arrangement is seen clearly in Fig. 3. The normalized values

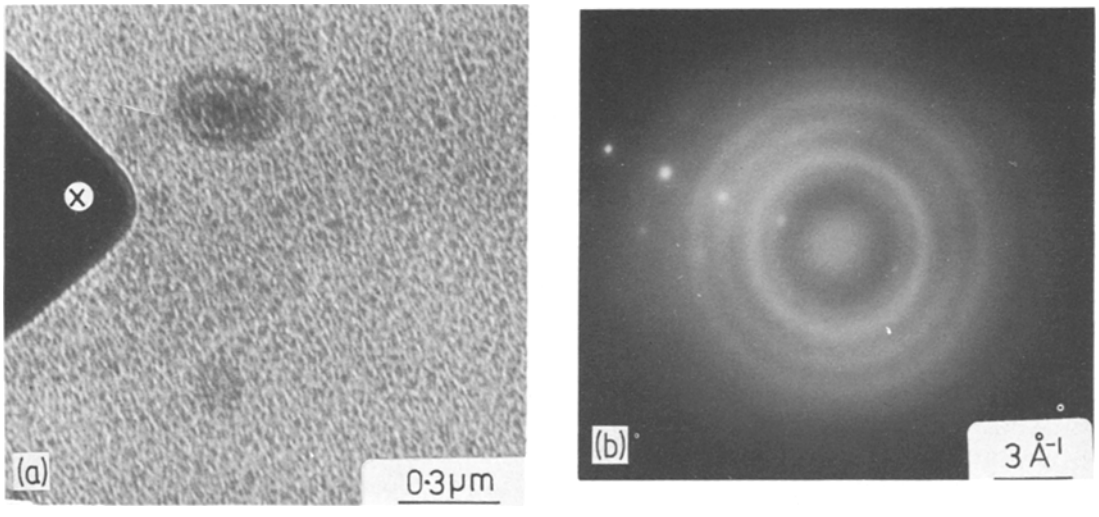

Figure 2 Showing (a) the microstructure and (b) the electron diffraction pattern of a film deposited at room temperature. The spots are from the superimposed [1 0 0] oriented NaCl crystal.

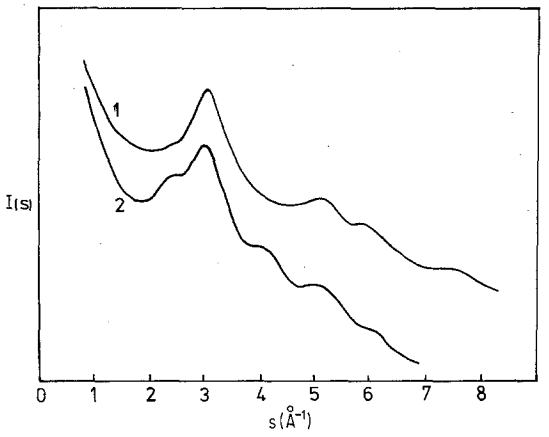

Figure 3 The diffracted intensities I (s) for an amorphous film deposited at 77 K (1) and a crystalline film deposited at room temperature (2).

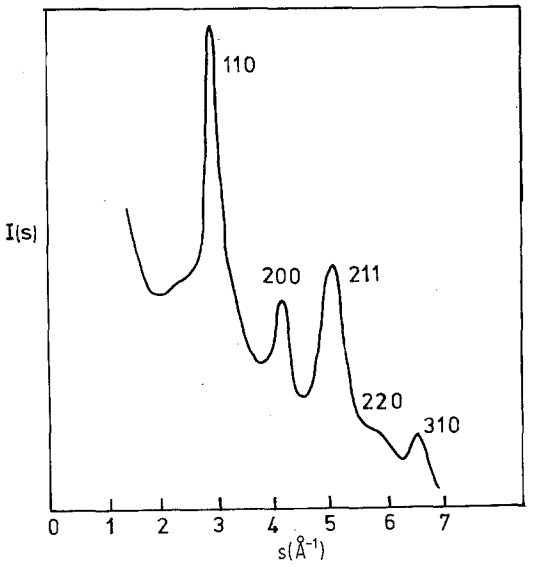

Figure 4 The diffracted intensity I (s) for an amorphous film crystallized at ~ 800° C. The peaks are labelled with the corresponding Miller indices.

s_n/s_1 should be noted in Table I and should be compared with ratios obtained from other non-crystalline systems and calculated for atomic models constructed in terms of schemes of dense random packing of hard spheres. The distinction between the amorphous and crystalline films is obvious and the close agreement between the form of the interference function or scattered intensity from the amorphous films studied here and elsewhere and the model calculations is clear. The films deposited onto the cold substrates are amorphous and metastable at room temperature whereas those grown on the room temperature substrates are crystalline with a two phase crystal structure.

The compositions of the films were determined by X-ray energy dispersive analysis and in all cases where found to be close to 76% Fe, 18% Cr and 8% Ni. This composition represents a depletion of Ni and enrichment of Fe in the films. No reason for this is known and no analysis of the minor constituents was attempted.

The metastability of the amorphous films was investigated by annealing the films in the TEM. No obvious changes in the diffraction pattern of these films occured until above 800 to 900° C when crystallization into a predominantly b c c phase occurred, Figs. 3 and 4. The grain size after crystallization was again small and of the order of 2.5 nm. The as-deposited crystalline films also experienced changes in this temperature range, including grain growth and a clearer definition of the mixed phase structure with what appeared to be a predominance of the f c c phase.

It is clear from this study that amorphous Fe–Cr–Ni based alloys can be prepared by sputtering onto substrates cooled to liquid nitrogen temperatures. What role gaseous impurities, such as occluded argon and oxygen, which may be at considerable concentrations play in the stabilization of the amorphous phase is not clear. Such an investigation is a subject for future study.

The electrochemical properties of these films prepared as coatings would be of interest and the measurements by Hashimoto *et al.* [3] on alloys quenched from the liquid phase suggest that amorphous coatings of the kind prepared here may provide attractive corrosion properties for suitable substrates.

Acknowledgements

The authors would like to thank Dr G. Slattery Ms S. Green (both of RNPD Laboratories, UKAEA) for the provision of EDAX facilities and for the analysis of the films.

References

1. N. J. GRANT and B. C. GIESSEN, "Rapidly Quenched Metals", (M.I.T. Press, Cambridge, Mass., USA, 1977).
2. R. HASEGAWA, R. C. O'HANDLEY and L. I.

MENDELSOHN, A. I. P. Conference Proceedings **34** (1976) 298.
3. K. HASHIMOTO, K. OSADA, T. MASUMOTO and S. SHIMODAIRA, *Corrosion Sci.* **16** (1976) 71.
4. *Idem, ibid* **16** (1976) 909.
5. *Idem, ibid* **16** (1976) 935.
6. S. S. NANDRA and P. J. GRUNDY, *Phys. Stat. Sol.* (a) **41** (1977) 65.
7. V. ASHWORTH, D. BAXTER, W. A. GRANT, R. P. M. PROCTOR and T. C. WELLINGTON, Proceedings of the International Conference on Ion Implantation in Semiconductors and Other Materials, 1974 (Plenum Press, New York, 1975) p. 367.
8. W. A. GRANT and J. S. WILLIAMS, *Sci. Prog. Oxf.* **63** (1976) 27.
9. A. ALI, W. A. GRANT and P. J. GRUNDY, *Rad. Effects* (to be published).
10. B. NAVINSEK, *Thin Solid Films* **13** (1972) 367.
11. W. A. NOWAK, *Mater. Sci. and Eng.* **23** (1976) 301.
12. N. J. SHEVCHIK, *J. Non-Cryst. Solids* **12** (1972) 141.
13. T. ICHIKAWA, *Phys. Stat. Sol.* (a) **19** (1973) 707.
14. L. B. DAVIES and P. J. GRUNDY, *Phys. Stat. Sol. (a)* **8** (1971) 189.
15. J. G. WRIGHT, *Inst. Phys. Conf. Ser.* **30** (1977) 251.
16. P. MRAFKO and P. DUHAJ, *J. Non-Cryst. Solids* **17** (1975) 143.

Received 5 July
and accepted 2 August 1977.

P. J. GRUNDY
J. M. MARSH*
Department of Pure and Applied Physics, University of Salford, UK

*Present address: Data Systems Div., Pilkington Bros Ltd., St. Helens, Merseyside.

Orientation dependence of l-alanine incorporation in TGS crystals

Ferroelectric triglycine sulphate (TGS) crystals are presently grown on a large scale so that the pyroelectric properties of this material may be utilized in single and multi-element infra-red detectors, and in the pyroelectric vidicon thermal imaging device. The crystals are grown from aqueous solution on seeds which are cut and cleaved from existing crystals perpendicular to the ferroelectric *b*-axis and which have a growth face area $\sim 1\,cm^2$. The seeds are mounted with silicone rubber on large horizontal perspex plates carried on each end of four cross-pieces on a central, reversing stirrer. Because each seed is set into the plate so that the single exposed face {0 1 0} is flush with the top surface, growth perpendicular to the plane of the seed can only take place vertically upwards, and the grown cystal is a truncated pyramid, with its base resting on the seed plate. This crystal is effectively one half of the crystal which would have grown had the seed been suspended freely in the solution.

TGS has the space group $P2_1/m$ above its Curie point (49.5° C) and the transition to the ferroelectric state is order/disorder, brought about principally by the switching of glycinium ions at one type of site in the lattice [1]. In an unpoled TGS crystal, with equal numbers of positive and negative domain terminations at an {0 1 0} surface, the mirror plane persists macroscopically at temperatures below the Curie point and the positive coordinate end of the *b*-axis is indistinguishable from the negative end. In practice this means that the crystal grown on one {0 1 0} face of a cleaved seed is the mirror image of the crystal grown on the opposite $\{0\,\bar{1}\,0\}$ face, but is otherwise identical. Thus the orientation of a seed mounted for growth need not be specified for pure TGS solutions.

It has been found [2] that it is advantageous to grow TGS crystals from solutions doped with *l*-alanine since the alanine substitutes to a small extent for glycine in the lattice and, because it has an asymmetric molecule, causes the ferroelectric domains to be locked in a single direction; this effect can be expressed in terms of the field required to overcome domain locking, which is known as the internal bias field. Since the crystal is permanently poled the plane of symmetry perpendicular to the *b*-axis no longer exists.

It would seem, *a priori*, that the alanine concentration in the growth solution would govern the proportion incorporated by crystals and hence their internal bias but the growth of alanine doped crystals of a required bias on {0 1 0} seeds was complicated by the fact that, as has been reported [3], TGS crystals grown from solutions containing *l*-alanine developed a habit which was asymmetric about the (0 1 0) plane. Seeds mounted with one orientation gave crystals whose growth rate was extremely slow (compared to the growth rate in comparable conditions in an undoped solution)